Accepted Manuscript

One-pot synthesis of strongly fluorescent DNA-$CuInS_2$ quantum dots for label-free and ultrasensitive detection of *anthrax lethal factor* DNA

Ziping Liu, Xingguang Su

PII: S0003-2670(16)31047-9

DOI: 10.1016/j.aca.2016.09.004

Reference: ACA 234784

To appear in: *Analytica Chimica Acta*

Received Date: 19 July 2016

Revised Date: 30 August 2016

Accepted Date: 1 September 2016

Please cite this article as: Z. Liu, X. Su, One-pot synthesis of strongly fluorescent DNA-$CuInS_2$ quantum dots for label-free and ultrasensitive detection of *anthrax lethal factor* DNA, *Analytica Chimica Acta* (2016), doi: 10.1016/j.aca.2016.09.004.

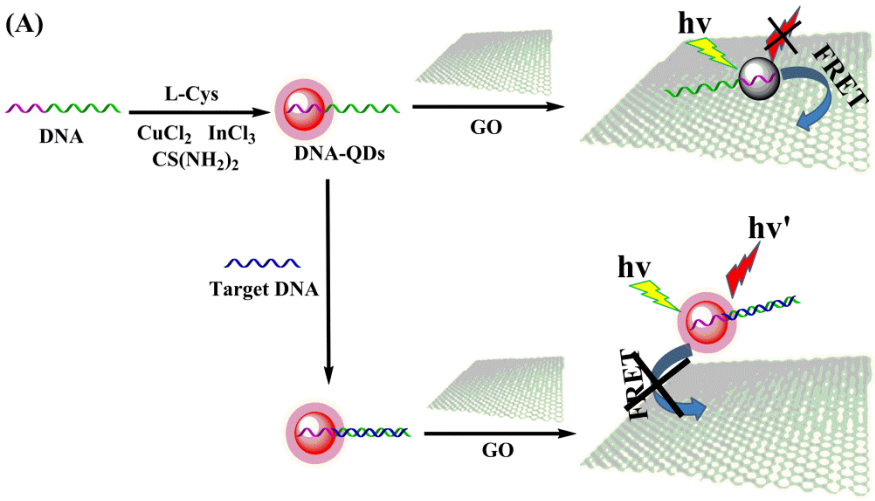
(A)
DNA
L-Cys
$CuCl_2$ $InCl_3$
$CS(NH_2)_2$
DNA-QDs
GO
hv
FRET
Target DNA
hv'
hv
FRET
GO

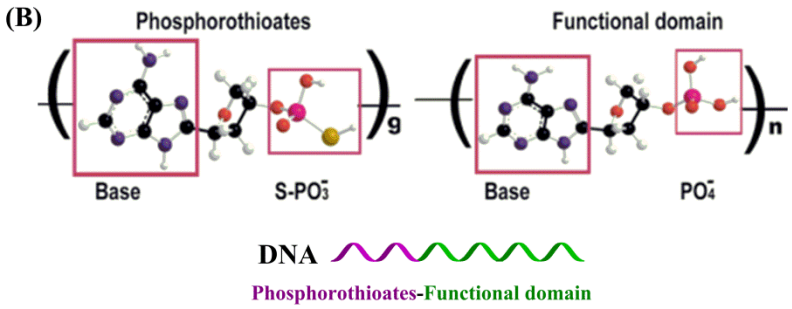
(B)
Phosphorothioates
Functional domain
Base
S-PO3
Base
PO4
9
n
DNA
Phosphorothioates-Functional domain

One-pot synthesis of strongly fluorescent DNA-$CuInS_2$ quantum dots for label-free and ultrasensitive detection of *anthrax lethal factor* DNA

Ziping Liu[a] and Xingguang Su[a*]

[a] *Department of Analytical Chemistry, College of Chemistry, Jilin University, Changchun 130012, China*

*Corresponding author

Tel.: +86-431-85168352

E-mail address: suxg@jlu.edu.cn

Abstract

Herein, high quality DNA-$CuInS_2$ QDs are facilely synthesized through a one-pot hydrothermal method with fluorescence quantum yield as high as 23.4%, and the strongly fluorescent DNA-$CuInS_2$ QDs have been utilized as a novel fluorescent biosensor for label-free and ultrasensitive detection of *anthrax lethal factor* DNA. L-Cysteine (L-Cys) and a specific-sequence DNA are used as co-ligands to stabilize the $CuInS_2$ QDs. The specific-sequence DNA consists of two domains: phosphorothiolates domain (sulfur-containing variants of the usual phosphodiester backbone) controls the nanocrystal passivation and serves as a ligand, and the functional domain (non-phosphorothioates) controls the biorecognition. The as-prepared DNA-$CuInS_2$ QDs have high stability, good water-solubility and low toxicity. Under the optimized conditions, a linear correlation was established between the fluorescence intensity ratio I/I_0 (I_0 is the original fluorescence intensity of DNA-$CuInS_2$ QDs, and I is the fluorescence intensity of DNA-$CuInS_2$ QDs/GO with the addition of various concentrations of *anthrax lethal factor* DNA) and the concentration of *anthrax lethal factor* DNA in the range of 0.029-0.733 nmol•L^{-1} with a detection limit of 0.013 nmol•L^{-1}. The proposed method has been successfully applied to the determination of *anthrax lethal factor* DNA sequence in human serum samples with satisfactory results. Because of low toxicity and fine biocompatibility, DNA-$CuInS_2$ QDs also hold potential applications in bioimaging.

Keywords: Fluorescence biosensor; DNA-QDs; *Anthrax lethal factor* DNA; Graphene oxide; One-pot synthesis

1. Introduction

Fluorescence strategies are commonly used as one of the most potent tools for bio-sensing, biological imaging and drug delivery because of their simplicity, speediness, high sensitivity, efficiency as well as high-throughput screening [1-6]. During the past decades, as a novel class of fluorescent nanomaterials, semiconductor quantum dot (QD)-based fluorescent sensors and sensing systems have invited tremendous attention owing to their extraordinary optoelectronic properties including high quantum yields, long fluorescence lifetimes, large extinction coefficients, pronounced photostability, broad absorption spectra coupled with narrow photoluminescent emission spectra as well as their small size [7-12]. Among the QD-based sensors and sensing systems, functionalized QD-based chemical and biochemical sensors and sensing systems are expected to open new opportunities in a new generation of detection, microelectronics, biomedicine and so on [13-15].

Functionalized QDs, which are modified and doped with biomolecules, have widely extended the applications of QDs in the areas of fluorescence bio-sensing, immunoassays and bio-imaging. DNA-labeled QDs are among the most studied functionalized QDs and have shown attractive properties for their biological use due to their high photostability, remarkable fluorescence properties, specific targeting, good water solubility, excellent cell membrane permeability and biocompatibility [16,17]. A common approach to obtain DNA-labeled QDs is via the selective and strong streptavidin-biotin coupling interaction between streptavidin QDs and biotin-appended DNA [18]. Although the method is convenient, the cross-linking and large size of streptavidin coated QDs are unfavorable for biological applications [19,20], because the optimal QDs for biological use have continuous light emission and exhibit a size of＜15 nm as well as low

cytotoxicity [21]. Additionally, it is difficult to control the binding site of a given biotin unit and the orientation of the biotin-DNA on the QDs, because streptavidin has four binding sites. Also, streptavidin QDs are expensive. DNA covalent conjugated with QDs through reaction between the amino/carboxy groups modified DNA and carboxy/amino groups of QDs can overcome these drawbacks [22]. However, the multistep process is time- and labour-intensive, and the acidic coupling conditions might cause the breakdown of the QDs. Thus, it is also out of reach of many researchers who want to use luminescent QDs as customized lumiphores.

Since Ma and co-workers first reported a one-step DNA-programmed synthesis of nanocrystals [23], several papers concerning DNA ligands for the aqueous synthesis of QDs have been published [24]. However, so far, the majority of the QD-based DNA-templated synthesis reports mainly focus on the QDs that containing heavy metals such as cadmium, lead, mercury and silver [25], which ultimately result in cytotoxicity and environmental problem owing to the leakage of heavy metal elements [26,27]. Especially, these QDs are sensitive to ambient conditions (e.g. heat, chemical, and photochemical disturbances), which makes them difficult to functionalize with DNA and lead to low output, low quantum yield and severely hampers their application. In the recent years, as newly emerging promising QDs, the environmentally friendly I-III-VI $CuInS_2$ QDs have attracted increasing research interests in bio-sensing and bio-imaging both in vitro and in vivo. This is not only due to their low toxicity that does not contain any toxic class A elements (Cd, Pb, and Hg) or class B elements (Se and As) compared with traditional semiconductor QDs, but also due to their NIR fluorescence signal (generally wavelengths>650 nm), which can avoid interferences from biological media, mainly tissue auto-fluorescence and scattering light [28].

Graphene oxide (GO) has attracted raised concerns because of its extraordinary mechanical,

thermal, chemical and optical properties as well as potential applications [29-31]. Rich of oxygen-containing groups on its surface, including carboxyl, hydroxyl and epoxy groups, GO is capable of good water-solubility, unique DNA adsorbing ability and wide-range energy transfer properties, which make it a wide prospect for biological application [32]. GO has π-systems and the sp^2 aromatic domains within GO can induce efficient fluorescence quenching via förster resonance energy transfer or non-radiative dipole-dipole coupling, which is critical for the sensitivity of assays [33-35]. Of our particular interest is the unique DNA/GO interactions in combination with the quenching properties of GO, which forms the basis of a convenient and versatile strategy for multicolor fluorescent DNA analysis. Some important works have been reported to achieve detection of different DNA targets. For example, Lu *et al.* reported that GO could bind and quench a dye-labeled single-stranded DNA (ssDNA) probe; the fluorescence was recovered when the probe formed a duplex with its target, which released the probe from GO [36]. Using a similar strategy based on GO and dye-labeled probes, He *et al.* reported a GO-based multicolor fluorescent DNA nanoprobe with different dyes as fluorophores that allows rapid and sensitive detection of multiplex DNA targets [37]. These prior researches focused on detection of targets or species with dye-labeled probes. However, organic dyes as fluorophores in the probes have non-negligible disadvantages such as poor photostability, easy photobleaching, and small Stokes shifts. To overcome these problems, *Qian et al.* developed several fluorescence assays for multiple DNA targets and different biological species using graphene quantum dots instead of dyes [38-40]. Nevertheless, tediously labeling or modifying processes still do not qualify them as excellent fluorophores of probes for biomolecules, which prompts scientists to investigate and exploit alternative fluorescent materials with good biocompatibility.

With regard to this, in this work, toxic heavy metal-free strongly fluorescent DNA-$CuInS_2$ QDs are synthesized by a one-step hydrothermal synthesis method for the first time, and a FRET biosensor for specific oligonucleotide sequence is established using the as-prepared $CuInS_2$ QDs as the energy donor and GO as the acceptor. The *anthrax lethal factor* DNA, coming from a Gram-positive spore-forming bacillus anthracis, has been chosen as a model target sequence [41-44]. It is considered to be one of the most potent and dangerous bioterrorist and biowarfare agents, as shown by the anthrax letter attacks in the fall of 2001 [45]. And it plays a key role in anthrax pathogenesis and is chiefly responsible for anthrax-related toxemia and host death, partly via inactivation of mitogen-activated protein kinase kinase (MAPKK) enzymes and consequent disruption of key cellular signaling pathways [46]. To the best of our knowledge, the novel one-step synthesized DNA-$CuInS_2$ QDs-based biosensor for label-free and ultrasensitive detection of *anthrax lethal factor* DNA hasn't been described before.

2. Experimental section

2.1 Materials and apparatus

All chemicals and reagents were of at least analytical reagent grade and used as-received without any further purification. The water used in all experiments had a resistivity higher than 18 $M\Omega \bullet cm^{-1}$. Copper (II) chloride dehydrate ($CuCl_2 \bullet 2H_2O$), indium (III) chloride tetrahydrate ($InCl_3 \bullet 4H_2O$) and sulfourea ($CS(NH_2)_2$) were purchased from Sigma-Aldrich Corporation. L-Cys, sodium chloride (NaCl), sodium hydroxide (NaOH), sodium dehydrogenized phosphate (NaH_2PO_4), disodium hydrogen phosphate (Na_2HPO_4), sodium phosphate (Na_3PO_4), rhodamine B and the other chemicals used were all purchased from Beijing Dingguo Changsheng Biotechnology Co. Ltd. All the oligonucleotide sequences used in the study were custom-made by

Shanghai Sangon Biotechnology Co. Ltd. The oligonucleotide sequences were listed in Table S1.

The hydro-thermal synthesis experiments were accomplished in a JCZ-JL intelligent digital display drum wind drying oven. All the fluorescence measurements were performed on a Shimadzu RF-5301 PC spectrofluorophotometer (Shimadzu Co., Kyoto, Japan) equipped with a xenon lamp using right-angle geometry. A 1 cm path-length quartz cuvette was used in all experiments. UV-vis absorption spectra were obtained using a Varian GBC Cintra 10e UV-vis spectrometer. Transmission electron microscopy (TEM) experiments were performed on a Philips Tecnai F20 TEM operating at 200 kV. FT-IR spectra were recorded with a Bruker IFS66V FT-IR spectrometer equipped with a DGTS detector (32 scans). The ultrasonic processes was proceeded on a KQ2200 ultrasonic cleaner (Ultrasonic instrument Co., Kunshan, China). The centrifugation processes were performed on a TGL-16G (Anke Technology Instrument Co., Shanghai, China). The shaking processes were performed on a HY-2 variable-speed reciprocal shaker (Guo Hua Electric Appliance Co., Changzhou, China). All pH measurements were completeed on a PHS-3C pH meter (Tuopu Co., Hangzhou, China). Fluorescence decays was conducted using a Fluorescence Lifetime and Steady State Spectroscopy (FLS920, Edinburgh Instrument).

2.2 One-pot synthesis of DNA-$CuInS_2$ QDs

The DNA-$CuInS_2$ QDs solution was synthesized by a one-step route via a hydrothermal synthesis method described in previous reports [23,47]. The modified DNA and L-Cys are both the stabilizing reagents. In a typical synthetic route, L-cys (3.60 mmol) was dissolved in 7.5 mL distilled water. Sequentially, DNA solution (0.067 μmol) was added into the above solution. Next, $CuCl_2$•$2H_2O$ (0.15 mmol) and $InCl_3$•$4H_2O$ (0.15 mmol) were injected into the solution and the solution turned light green. The pH value of the mixture solution was then adjusted to 11.3 by

adding 4 mol•L^{-1} NaOH solution with stirring. During this process, the solution changed from light green to clear brown. After stirring for 10 min, CS(NH2)2 (0.30 mmol) was added to the mixture. The Cu-to-In-to-S and Cu-to-L-cys ratios were 1:1:2 and 1:24, respectively. All the above mentioned experimental procedures were performed at room temperature, and then the solution was transferred into a Teflon-lined stainless steel autoclave with a volume of 15 mL. The autoclave was maintained at 150℃ for 23 h and then cooled down to room temperature by a natural cooling process. The obtained yellow-brown DNA-$CuInS_2$ QDs solution was centrifuged at a speed of 10000 rpm at room temperature for 20 min to remove the black deposit. The upper yellow-brown solution was dialyzed in the membrane tubing with a molecular weight cut-off of 3 kDa against ultrapure water to remove small molecules and ions. The as-prepared DNA-$CuInS_2$ QDs solution could be precipitated by ethanol, and the precipitate was isolated by centrifugation, washed with ethanol several times, then the powder was dried at 50 ℃ for 24 h. The obtained powder was used for characterization.

2.3 Quantum yields (QYs) measurements of DNA-$CuInS_2$ QDs

QYs of the DNA-$CuInS_2$ QDs were measured by using rhodamine B in water as the reference standard (QY=0.31) [48], and then the QYs were calculated according to the following equation:

$$\phi_x = \phi_{st}(I_x / I_{st})(\eta_x^2 / \eta_{st}^2)(A_{st} / A_x) \qquad (1)$$

Where φ is the quantum yield, I is the measured integrated emission intensity, η is the refractive index of the solvent, and A is the optical density. The subscript "st" refers to standard with known quantum yield and "x" for the sample. In order to minimize re-absorption effects, absorption in the 1 cm fluorescence cuvette was kept below 0.10.

2.4 Preparation of GO

GO used in this study was synthesized according to modified Hummer's method [49]. In a typical experiment, 2 g graphite powder was dispersed in 44 mL concentrated H_2SO_4, and incubated for 15 min in the ice-water bath. 6 g $KMnO_4$ was then added gradually into the solution under stirring with the temperature below 20 ℃. This mixed solution was stirred at 15 ℃ for 20 min and reacted at 35 ℃ for 1 h. Subsequently, 160 mL deionized water was dropwise added to dilute the mixture. The resulting mixture was kept at 60 ℃ for 15 min, 200 mL water and 20 mL 30% H_2O_2 were then added to end the reaction. The product was washed with deionized water to remove the acid, and was further purified by dialysis for 2 week to remove the remaining metal species. Exfoliation was taken out by sonicating GO under ambient conditions. The obtained dispersion was centrifuged at 5000 rpm to remove any unexfoliated GO. The concentration of GO stock solution is 1.88 mg•mL^{-1}.

2.5 Fluorescence measurement of anthrax lethal factor DNA

The *anthrax lethal factor* DNA detection process was carried out as follows: 200 μL DNA-$CuInS_2$ QDs, different concentrations of target DNA T1 (*anthrax lethal factor* DNA) and 10 μL GO were respectively added into a 2.0 mL calibrated centrifuge tube. Then the solution was diluted to 2.0 mL with NaH_2PO_4-Na_2HPO_4 buffer solution (0.01 mol•L^{-1}, pH 7.4). At an excitation wavelength of 590 nm, the fluorescence emission spectra of dsDNA-QDs/GO system were recorded in the 610-800 nm emission wavelength range and used for quantitative analysis.

2.6 Detection of anthrax lethal factor DNA in human serum samples

In real sample assay, three fresh human blood samples were collected from healthy volunteer through venipuncture at the Hospital of Changchun China, Japan Union Hospital. All experiments were performed in compliance with the relevant laws and institutional guidelines, and the writing

of informed consent for all samples was obtained from human subjects. Some necessary processes were conducted to remove impurities to get the human serum samples before carrying out fluorescence experiments. Firstly, the blood samples were segregated by adding acetonitrile (the volume of acetonitrile and blood was 1.5: 1) and centrifuged at 10,000 rpm for 10 min after stored for one night at room temperature. Then, all supernatant serum samples were subjected to a 100-fold dilution with NaH_2PO_4-Na_2HPO_4 buffer solution before analysis, and a certain concentration of *anthrax lethal factor* DNA was added to prepare the spiked samples. Detection processes were carried out according to the above mentioned optimized conditions for *anthrax lethal factor* DNA detection.

3. Results and discussion

3.1 The strategy for the detection of anthrax lethal factor DNA

The design strategy of the present work is illustrated in Scheme 1. Scheme 1 (A) shows the preparation of DNA-$CuInS_2$ QDs by a one-step hydrothermal synthesis method. L-Cys and a specific-sequence DNA compounds were used as co-ligands to stabilize the QDs. The DNA ligand consisted of two domains: phosphorothiolates (sulfur-containing variants of the usual phosphodiester backbone, which preferentially bind to the QDs surface over phosphates) controls the nanocrystal passivation, and the functional part (non-phosphorothioates), which is available for specifically bind to DNA, proteins or cells that have unique surface recognition markers [50]. Structures of the phosphorothioates and functional domain had been given in Scheme 1 (B). The surface reactivity of DNA sequences is crucial for the growth and the quality of QDs, as previously reported. Carbonyl groups and amine groups are responsible for surface passivation, secondary conformation and/or steric effects of the capping sequence strands play a significant

role in stabilizing the nanocrystals [51,52]. In the synthesis process, the DNA-$CuInS_2$ QDs were gradually formed. The S atoms in the phosphorothioates domain of the designed DNA were inserted into DNA-$CuInS_2$ QDs, while the functional domain (non-phosphorothioates) extended away from the surfaces of DNA-$CuInS_2$ QDs and was available for recognizing the target molecule or protein.

Then, the as-prepared DNA-$CuInS_2$ QDs were used in the analytical detection of *anthrax lethal factor* DNA, as shown in Scheme 1 (A). The bio-sensing platform was established based on the different adsorption properties of GO towards ssDNA in comparison with that of double-stranded DNA (dsDNA). According to the literature, GO can act as a "nanoscaffold" for ssDNA, because the nucleobases of the ssDNA are uncoiled partially and can be exposed to GO [53]. However, the formation of double-stranded DNA (dsDNA) reduces the exposure of the nucleobases, which weakens the π-π stacking interaction [54]. In this paper, the DNA-$CuInS_2$ QDs spontaneously absorbed onto the surface of GO by means of π-π stacking interaction and hydrogen bonding interaction between hydroxyl/amine groups of ssDNA and hydroxyl/carboxyl groups of GO [55]. Such interactions brought the fluorescence DNA-$CuInS_2$ QDs in close proximity to the GO surface, and led to the fluorescence of ssDNA-QDs quenched owing to förster resonance energy transfer from DNA-$CuInS_2$ QDs to GO. In the presence of *anthrax lethal factor* DNA, the DNA-$CuInS_2$ QDs would preferentially bind with the *anthrax lethal factor* DNA, forcing DNA-$CuInS_2$ QDs to undergo a conformational change and form a self-hybridized dsDNA-$CuInS_2$ QDs complex. In the dsDNA complex, the nucleobases were hidden inside the helical structure, and then the non-covalent π-π stacking and hydrogen-bonding interactions between DNA-$CuInS_2$ QDs and GO were impaired [56]. By this way, the DNA-$CuInS_2$ QDs were

released from the GO sheet and the fluorescence was restored. Thus, the determination of *anthrax lethal factor* DNA could be achieved by taking advantage of the different adsorption properties of GO towards ssDNA in comparison with that of dsDNA.

Fig.1 (A) and (B) showed the Transmission Electron Microscopy (TEM) images of the $CuInS_2$ QDs and as-prepared DNA-$CuInS_2$ QDs, respectively. Inset is the amplification of a single particle. From the TEM images, it can be seen that the DNA-$CuInS_2$ QDs were spherical particles and well dispersible in aqueous solution, which is better than that of $CuInS_2$ QDs. Fig.1 (C) and Fig.1 (D) were the granulometric distribution of $CuInS_2$ QDs and DNA-$CuInS_2$ QDs, respectively. From Fig.1 (C), it can be seen that $CuInS_2$ QDs dispersed from 1 nm to 5 nm with an average diameter of 3.23 nm. From Fig.1 (D), it can be seen that DNA-$CuInS_2$ QDs are nearly monodispersed with the diameter from 2 nm to 4 nm, and revealed an average particle size of 3.37 nm. Fig.1 (E) depicted the UV-Vis absorption spectra and normalized fluorescence emission spectra of the $CuInS_2$ QDs (dash line) and DNA-$CuInS_2$ QDs (solid line). It can be observed that DNA-$CuInS_2$ QDs and $CuInS_2$ QDs shows similar UV-Vis absorption and fluorescence emission spectra, but the fluorescence intensity of DNA-$CuInS_2$ QDs is obviously enhanced in comparison with that of $CuInS_2$ QDs, which might be attribute to the surface reactivity of the capping sequences that mainly influences the quality of nanocrystals [51,52]. Moreover, the fluorescence spectrum of the DNA-$CuInS_2$ QDs is blue-shifted by 3 nm (from 655 nm to 652 nm) compared with $CuInS_2$ QDs (L-Cys as the ligand alone) under the same synthesis conditions. This phenomenon indicates that the DNA ligand may interact electronically with the crystal surface and alter its electronic properties [23]. Fig.1 (F) is the photographs of $CuInS_2$ QDs (left) and DNA-$CuInS_2$ QDs (right) under UV light, respectively. It can be seen that the luminescence signal of DNA-$CuInS_2$ QDs is

brighter than that of $CuInS_2$ QDs. Using rhodamine B as a reference, the fluorescence quantum yield of the prepared DNA-$CuInS_2$ QDs is measured to be 23.4% (Fig. S1), which is much higher than that of $CuInS_2$ QDs (3.5%). This result is because of the formation of the L-cys and DNA co-ligands, which can offset the surface defect of $CuInS_2$ QDs. The time-decay curves were conducted to further confirm their difference from their lifetime (Fig. S2). The decay curves can be fitted to a biexponential model, and the average fluorescence lifetime of $CuInS_2$ QDs and DNA-$CuInS_2$ QDs were 127.0 and 155.5 ns, respectively. The fluorescence lifetime of DNA-$CuInS_2$ QDs was longer than that of $CuInS_2$ QDs, indicating that the as-prepared DNA-$CuInS_2$ QDs had superior fluorescent properties [23].

The FT-IR spectra of the $CuInS_2$ QDs with L-Cys as stabilizers and DNA-$CuInS_2$ QDs with L-Cys and DNA as co-stabilizers were compared to confirm the coordination of the DNA sequences on the surface of the DNA-$CuInS_2$ QDs. As shown in Fig. 2 (green curve), the majority of L-Cys functional groups could be clearly found through the broad O-H stretching vibration (3410 cm^{-1}), the characteristic peaks of -COOH (1470 cm^{-1} symmetric stretching vibration) and the characteristic peaks of $-NH_2$ (1640 cm^{-1}). We could ascertain that the original $CuInS_2$ QDs were capped by L-Cys. From the red curve in Fig. 2, the majority of the DNA sequences functional groups can be clearly found through the stretching vibrations of C=O (1580 cm^{-1}), the out of phase symmetrical stretches (1060 cm^{-1}) and the P-O stretches of the main chain (930 cm^{-1}), while these characteristic peaks were not observed in the FT-IR spectra of $CuInS_2$ QDs (Fig. 2 green curve). These results further demonstrated that the DNA-$CuInS_2$ QDs had been successfully prepared.

To further explore the potential applications of DNA-$CuInS_2$ QDs in bio-sensing, one of the

primary requirements is water-solubility and stability under various pH and ionic environments. The DNA-$CuInS_2$ QDs with abundant hydroxyl, amino and carboxyl groups inherently has good solubility in water. Their stability in various environments was further investigated, as shown in Fig. 3. Fig. 3 (A) was the photostability result. The DNA-$CuInS_2$ QDs solution was irradiated continuously over a period of 60 min and displayed a high photostability. Fig. 3 (B) suggested that the fluorescence intensity of the as-prepared DNA-$CuInS_2$ QDs solution remained almost the same in different pH environments. This is very different from many other water-soluble fluorescence dyes and QDs, which usually exhibit obvious decrease in fluorescence emission with decreased pH values and poor fluorescence and photostability in acidic medium. Furthermore, the effect of salt concentration on the fluorescence of DNA-$CuInS_2$ QDs after incubation of 60 min was investigated. As shown in Fig. 3 (C), it can be found that the DNA-$CuInS_2$ QDs were also highly stable in a wide salt concentration of 0-100 mmol•L^{-1}. The high stability of DNA-$CuInS_2$ QDs is a significant merit in bio-sensing applications.

Fig. 4 showed the fluorescence emission spectra of DNA-$CuInS_2$ QDs (curve a), the ssDNA-$CuInS_2$ QDs/GO complexes (curve b) and the dsDNA-$CuInS_2$ QDs/GO complexes (curve c). It can be seen that DNA-$CuInS_2$ QDs exhibited strong fluorescence emission with the maximum emission peak of 655 nm in the absence of GO. However, in the presence of GO (18.0 μg•mL^{-1}), the fluorescence intensity of DNA-$CuInS_2$ QDs decreased rapidly to7.6% of the original intensity, revealing the significantly high binding affinity of DNA-$CuInS_2$ QDs to GO and the strong quenching effect of GO on the fluorescence of DNA-$CuInS_2$ QDs. Upon being incubated with complementary target DNA T1 (*anthrax lethal factor* DNA) for 1 h prior to the addition of GO, the dsDNA-$CuInS_2$ QDs/GO mixture exhibited a higher fluorescence emission intensity,

which was about 68.2% of the original intensity of DNA-$CuInS_2$ QDs (curve c). Such results illustrated the low binding affinity of dsDNA-$CuInS_2$ QDs towards GO.

3.2 Optimization for anthrax lethal factor DNA detection

Before quantity analysis of *anthrax lethal factor* DNA using the as-prepared DNA-$CuInS_2$ QDs, we optimized the detection conditions including reaction time, pH, salt concentration and the concentration of GO. The kinetic behaviors of ssDNA-$CuInS_2$ QDs and dsDNA-$CuInS_2$ QDs in the presence of GO were firstly studied by monitoring fluorescence intensity as a function of time. Fig. 5 (A) showed that the fluorescence of free ssDNA-$CuInS_2$ QDs rapidly decreased and kept unchangeable in 20 min incubation time in the presence of GO, indicating that ssDNA-$CuInS_2$ QDs were adsorbed on the surface of GO completely within 20 min. Thus, 20 min was chose for the fluorescemce quenching experiments. Fig.5 (B) was the effect of incubation time on the fluorescence intensity of dsDNA-QDs with the addition of GO. From Fig. 5 (B), it can be observed that the fluorescence gradually increased and reached a plateau in 1 h incubation time. Therefore, 1 h incubating time was chose for target *anthrax lethal factor* DNA and DNA-$CuInS_2$ QDs.

The effect of pH on the sensing system was then studied over the range 5.4-11.4. It could be observed from Fig. 5 (C) that the relative fluorescence intensity I/I_0 (I_0 and I were the fluorescence intensity of ssDNA-$CuInS_2$ QDs/GO in the absence and presence of *anthrax lethal factor* DNA, respectively) was much bigger in neutral or acidic medium than that in alkaline medium, and reached the highest value at pH 7.4. As previously studies, ssDNA containing aromatic and hydrophobic rings could bind to GO via hydrophobic interactions and π-π stacking. Raising the pH may facilitate the deprotonation of the carboxyl groups on GO surface, which would increase

the electrostatic repulsion between the negatively charged GO and the polyanionic ssDNA [57-60]. Moreover, the increasing pH could weaken the electron-acceptor ability of the carboxyl groups of GO, which would further suppress the π-π stacking between DNA and GO. Next, the effect of salt concentration on the sensing system was studied. From Fig. 5 (D), it can be seen that the relative fluorescence intensity I/I_0 (I_0 and I were the fluorescence intensity of ssDNA-$CuInS_2$ QDs/GO in the absence and presence of *anthrax lethal factor* DNA, respectively) was the highest at 100 μmol•L^{-1} NaCl. Therefore, we chose 100 μmol•L^{-1} NaCl in this work.

Fig. 6 was the fluorescence spectra of DNA-$CuInS_2$ QDs in the presence of different concentration of GO over the range of 0-18.0 μg•mL^{-1}. As shown in Fig. 6, the original DNA-$CuInS_2$ QDs solution [200 μL in NaH_2PO_4-Na_2HPO_4 buffer solution (0.01 mol•L^{-1}, pH 7.4)] showed rather strong fluorescence, the fluorescence intensity of DNA-$CuInS_2$ QDs decreased gradually with the increasing of the concentration of GO in the range of 0-18.0 μg•mL^{-1}. The inset in Fig. 6 showed the relationship between the fluorescence intensity ratio I/I_0 (I_0 and I were the fluorescence intensity of DNA-$CuInS_2$ QDs in the absence and presence of GO, respectively) and the concentration of GO. It can be found that 18.0 μg•mL^{-1} GO presented a quenching effect of 92.4%. Based on previous reports, it is adequate to provide a low fluorescence background and high signal-to-background ratio, which can greatly enhance the sensitivity of the sensors [61-63].

3.3 Fluorescence detection of target DNA T1 (anthrax lethal factor DNA)

Fig. 7 (A) showed the fluorescence emission spectra of DNA-$CuInS_2$ QDs after incubation with different concentrations of target DNA T1 in the presence of GO under the optimum conditions. As shown in Fig. 7, the fluorescence intensity of the dsDNA-$CuInS_2$ QDs/GO system gradually increased with the increasing concentration of target DNA T1. Fig. 7 (B) demonstrates that there

was good linearity between the relative fluorescence intensity I/I_0 (I_0 is the original fluorescence intensity of DNA-$CuInS_2$ QDs, and I is the fluorescence intensity of DNA-$CuInS_2$ QDs/GO with the addition of various concentrations of DNA T1) and the concentration of target DNA T1 in the range of 0.029-0.733 nmol•L^{-1}. The regression equation could be described as follows:

$$I/I_0=0.138+0.775\ [T1],\ \text{nmol•}L^{-1} \qquad (2)$$

The corresponding regression coefficient (R^2) is 0.988, and the detection limit (LOD) for T1 was 0.013 nmol•L^{-1}. The detection limit is defined by the equation LOD=3σ/s, where σ is the standard deviation of the corrected blank signals of the ssDNA-$CuInS_2$ QDs/GO and s is the slope of the calibration curve. A comparison between the proposed method and other reported methods for *anthrax lethal factor* determination in linear range and LOD was summed up in Table S2. Compared with other methods, our method showed a comparable quantification range and LOD.

3.4 Sequence selectivity and interference study

Selectivity is a very important parameter to evaluate the performance of a new sensor, especially for a biosensor with potential applications in biological samples, a highly selective response to the target over other potentially competing species is necessary. Therefore, we firstly investigated the sequence selectivity of the designed fluorescent biosensor. Fig. 8 (A) showed the corresponding fluorescence intensity ratio (I/I_0) histograms in the presence of DNA target T1 (red bar), single-base-mismatched target DNA T2 (green bar) and two-base-mismatched target DNA T3 (blue bar). It can be observed that the fluorescence intensity ratio (I/I_0) obtained upon the addition of 0.733 nmol•L^{-1} T2 and T3 is about 54.8% and 26.4% of the fluorescence intensity ratio (I/I_0) obtained upon the addition of the same amount of T1, respectively. Such decrease indicated that the mismatched targets had lower hybridization ability toward DNA-$CuInS_2$ QDs compared to

the complementary target. Thus we can conclude that the designed sensing method has a higher selectivity and owns great promise for application in *anthrax lethal factor* DNA detection.

Then, we studies the interference effect of various coexisting substances including some common inorganic ions and important biologically molecules to our fluorescent biosensor. The results were showed in Fig. 8 (B). A relative error of ±5.0% was considered to be tolerable. The tolerable concentration ratios of coexisting substances to 0.733 nmol•L^{-1} *anthrax lethal factor* DNA was over 100 fold for K^+, Na^+, Ca^{2+}, Mg^{2+}, Zn^{2+}, acetate, Cl^-, SO_4^{2-}, CO_3^{2-}, citrate, glucose, BSA and HSA. From Fig. 8 (B), it can be seen that the present biosensor was insensitive to other potentially coexisting substances, that is, the coexisting substances had no significant influence on our developed biosensor.

3.5 Detection of target DNA in serum samples

In order to evaluate the feasibility of the proposed method in real sample detection, the developed detection system was applied for the determination of *anthrax lethal factor* in human serum samples. The human serum was diluted 100 times with deionized water and then adjusted to pH 7.4. Different concentrations of *anthrax lethal factor* DNA were added to the diluted serum samples to prepare the spiked samples. Then, the concentrations of *anthrax lethal factor* DNA in samples were determined by the standard addition method and the results were listed in Table 1. The accuracy of the proposed method was evaluated by determining the recovery of *anthrax lethal factor* DNA in real samples. It can be observed that the average recoveries of *anthrax lethal factor* DNA in the real samples were in the range of 96-105% and the RSD was lower than 3.5%. The above results demonstrated the potential applicability of the present method in real sample detection.

4. Conclusions

In conclusion, high quality DNA-$CuInS_2$ QDs with strongly fluorescence, good water-solubility, excellent stability and low toxicity have been prepared by a one-step hydrothermal method. The DNA-$CuInS_2$ QDs possess FL quantum yields as high as 23.4%. Moreover, the one-pot synthesized fluorescent DNA-$CuInS_2$ QDs are explored to utilize as a biosensor for label-free detection of target *anthrax lethal factor* DNA. The DNA-$CuInS_2$ QDs fluorescent sensor are significant for the following features: (1) The synthetic protocol reported here is very simple and facile, they can be directly synthesized by a one-pot method; (2) Compared with traditional Cd-containing semiconductor nanoparticles, the newly prepared DNA-$CuInS_2$ QDs are low toxicity; (3) The sensing system is straightforward and economic, only uses DNA-$CuInS_2$ QDs and ssDNA/dsDNA binding discrimination towards GO; (4) The fluorescent biosensor employs "turn off-on" switching mode, which possesses the advantages of low background interference and superior sensitivity and high selectivity. (5) The proposed method had been successfully applied to the determination of *anthrax lethal factor* DNA sequence in human serum samples with satisfactory results. It is expected that the DNA-$CuInS_2$ QDs-based sensing system can supply a universal sensing platform for the detection of other target molecules by simply changing the types of ssDNA sequences for different targets.

Acknowledgements

This work was financially supported by the National Natural Science Foundation of China (Nos. 21075050 and 21275063), the Science and Technology Development project of Jilin

province, China (No. 20150204010GX), and the Graduate Innovation Fund of Jilin University (2016070).

References

[1] P. Oh, Y. Li, J. Y. Yu, E. Durr, K. M. Krasinska, L. A. Carver, J. E. Testa, J. E. Schnitzer, Subtractive proteomic mapping of the endothelial surface in lung and solid tumours for tissue-specific therapy, Nature 429 (2004) 629-635.

[2] R. M. Hoffman, The multiple uses of fluorescent proteins to visualize cancer *in vivo,* Nat. Rev. Cancer 5 (2005) 796-806.

[3] X. Michalet, F. F. Pinaud, L. A. Bentolila, J. M. Tsay, S. Doose, J. J. Li, G. Sundaresan, A. M. Wu, S. S. Gambhir and S. Weiss, Quantum dots for live cells, in vivo imaging, and diagnostics, Science 307 (2005) 538-544.

[4] X. B. Zhang, C. H. Liu, H. H. Wang, H. Wang and Z. P. Li, Rare earth ion mediated fluorescence accumulation on a single microbead: an ultrasensitive strategy for the detection of protein kinase activity at the single-cell level, Angew. Chem. Int. Ed. 54 (2015) 15186-15190.

[5] J. Huang, H. Wang, X. H. Yang, Y. J. Yang, K. Quan, L. Ying, N. L. Xie, M. Ou and K. M. Wang, A supersandwich fluorescence in situ hybridization strategy for highly sensitive and selective mRNA imaging in tumor cells, Chem. Commun. 52 (2016) 370-373.

[6] X. Z. Wang, T. Hou, S. S. Dong, X. J. Liu, F. Li, Fluorescence biosensing strategy based on mercury ion-mediated DNA conformational switch and nicking enzyme-assisted cycling amplification for highly sensitive detection of carbamate pesticide, Biosensors and Bioelectronics 77 (2016) 644-649.

[7] R. Freeman, I. Willner, Optical molecular sensing with semiconductor quantum dots (QDs), Chem. Soc. Rev. 41 (2012) 4067-4085.

[8] X. Gao, J. Wu, X. Wei, C. He, X. Wang, G. Guo, Q. Pu, Facile one-step photochemical synthesis of water soluble CdTe(S) nanocrystals with high quantum yields, J. Mater. Chem. 22 (2012) 6367-6373.

[9] Y. Y. Zhao, Y. X. Ma, H. Li and L. Y. Wang, Composite QDs@MIP nanospheres for specific recognition and direct fluorescent quantification of pesticides in aqueous media, Anal. Chem. 84 (2012) 386-395.

[10] A. J. Morris-Cohen, M. Malicki, M. D. Peterson, J. W. J. Slavin and M. A. Weiss, Chemical, structural, and quantitative analysis of the ligand shells of colloidal quantum dots, Chem. Mater.

25 (2013) 1155-1165.

[11] L. Li, P. Wu, K. Hwang and Y. Lu, An exceptionally simple strategy for DNA-functionalized up-conversion nanoparticles as biocompatible agents for nanoassembly, DNA delivery, and imaging, J. Am. Chem. Soc. 135 (2013) 2411-2414.

[12] A. M. Jawaid, S. Chattopadhyay, D. J. Wink, L. E. Page and P. T. Snee, Cluster-seeded synthesis of doped CdSe:Cu_4 quantum dots, ACS Nano 7 (2013) 3190-3197.

[13] M. A. El-Sayed, Small is different: shape-, size-, and composition-dependent properties of some colloidal semiconductor nanocrystals, Acc. Chem. Res. 37 (2004) 326-333.

[14] I. L. Medintz, H. T. Uyeda, E. R. Goldman and H. Mattoussi, Quantum dot bioconjugates for imaging, labelling and sensing, Nat. Mater. 4 (2005) 435-446.

[15] H. Zhang, J. Han and B. Yang, Structural fabrication and functional modulation of nanoparticle–polymer composites, Adv. Funct. Mater. 20 (2010) 1533-1550.

[16] H. Wang, R. H. Yang, L. Yang, W. H. Tan, Nucleic acid conjugated nanomaterials for enhanced molecular recognition, ACS Nano 3 (2009) 2451-2460.

[17] L. Gao, N. Ma, DNA-templated semiconductor nanocrystal growth for controlled DNA packing and gene delivery, ACS Nano 6 (2012) 689-695.

[18] L. Z. Liu, H. Li, T. Qiu, G. H. Zhou, K. Y. Wong, Z. K. He, Z. H. Liu, Construction of a molecular beacon based on two-photon excited fluorescence resonance energy transfer with quantum dot as donor, Chem. Commun. 47 (2011) 2622-2624.

[19] I. L. Medintz, H. T. Uyeda, E. R. Goldman, H. Mattoussi, Quantum dot bioconjugates for imaging, labelling and sensing, Nat. Mater. 4 (2005) 435-446.

[20] P. Chan, T. Yuen, F. Ruf, J. Gonzalez-Maeso, S. C. Sealfon, Method for multiplex cellular detection of mRNAs using quantum dot fluorescent *in situ* hybridization, Nucleic Acids Res. 33 (2005) 1-8.

[21] A. M. Smith, S. M. Nie, Next-generation quantum dots, Nat. Biotechnol. 27 (2009) 332-333.

[22] S. P. Wang, N. Mamedova, N. A. Kotov, W. Chen, J. Studer, Antigen/antibody immunocomplex from CdTe nanoparticle bioconjugates, Nano Lett. 2 (2002) 817-822.

[23] N. Ma, E. H. Sargent, S. O. Kelley, One-step DNA-programmed growth of luminescent and biofunctionalized nanocrystals, Nat. Nanotechnol. 4 (2009) 121-125.

[24] N. Ma, S. O. Kelley, DNA-based programing of quantum dot properties, WIRES Nanomed. Nanobiotechnol. 5 (2013) 86-94.

[25] N. Chen, Y. He, Y. Y. Su, C. H. Fan, The cytotoxicity of cadmium-based quantum dots, Biomaterials 33 (2012) 1238-1244.

[26] R. Hardman, A toxicologic review of quantum dots: toxicity depends on physicochemical and environmental factors, Environ. Health Persp. 114 (2006) 165-172.

[27] Z. P. Liu, Q. Ma, X. Y. Wang, Z. H. Lin, H. Zhang, L. L. Liu, X. G. Su, A novel fluorescent nanosensor for detection of heparin and heparinase based on $CuInS_2$ quantum dots, Biosens. Bioelectron. 54 (2014) 617-622.

[28] R. G. Xie, M. Rutherford, X. G. Peng, Formation of high-quality I-III-VI semiconductor nanocrystals by tuning relative reactivity of cationic precursors, J. Am. Chem. Soc. 131 (2009) 5691-5697.

[29] G. Eda and M. Chhowalla, Chemically derived graphene oxide: towards large-area thin-film electronics and optoelectronics, Adv. Mater. 22 (2010) 2392-2415.

[30] K. P. Loh, Q. Bao, P. K. Ang and J. Yang, The chemistry of graphene, J. Mater. Chem. 20 (2010) 2277-2289.

[31] Y. Y. Guo, L. Deng, J. Li, S. Guo, E. Wang, S. Dong, Hemin-graphene hybrid nanosheets with intrinsic peroxidase-like activity for label-free colorimetric detection of single-nucleotide polymorphism, ACS Nano. 5 (2011) 1282-1290.

[32] D. R. Dreyer, S. Park, C. W. Bielawski, R. S. Ruoff, The chemistry of graphene oxide, Chem. Soc. Rev. 39 (2010) 228-240.

[33] C. H. Lu, H. H. Yang, C. L. Zhu, X. Chen, G. N. Chen, A graphene platform for sensing biomolecules, Angew. Chem. Int. Ed. 48 (2009) 4785-4787.

[34] S. P. Song, Y. Qin, Y. He, Q. Huang, C. H. Fan, H. Y. Chen, Functional nanoprobes for ultrasensitive detection of biomolecules, Chem. Soc. Rev. 39 (2010) 4234-4243.

[35] M. Zhang, B.-C. Yin, W. Tan, B.-C. Ye, A versatile graphene-based fluorescence "on/off" switch for multiplex detection of various targets, Biosens. Bioelectron. 26 (2011) 3260-3265.

[36] C. H. Lu, H. H. Yang, C. L. Zhu, X. Chen, G. N. Chen, A graphene platform for sensing biomolecules, Angew. Chem. Int. Ed. 48 (2009) 4785-4787.

[37] S. J. He, B. Song, D. Li, C. F. Zhu, W. P. Qi, Y. Q. Wen, L. H. Wang, S. P. Song, H. P. Fang, C. H. Fan, A graphene nanoprobe for rapid, sensitive, and multicolor fluorescent DNA analysis, Adv. Funct. Mater 20 (2010) 453-459.

[38] Z. S. Qian, X. Y. Shan, L. J. Chai, J. J. Ma, J. R. Chen and H. Feng, A universal fluorescence sensing strategy based on biocompatible graphene quantum dots and graphene oxide for the detection of DNA, Nanoscale 6 (2014) 5671-5674.

[39] Z. S. Qian, X. Y. Shan, L. J. Chai, J. R. Chen, H. Feng, Simultaneous detection of multiple DNA targets by integrating dual-color graphene quantum dot nanoprobes and carbon nanotubes, Chem. Eur. J. 20 (2014) 16065-16069.

[40] Z. S. Qian, X. Y. Shan, L. J. Chai, J. R. Chen, H. Feng, Dual-colored graphene quantum dotslabeled nanoprobes/graphene oxide: functional carbon materials for respective and simultaneous detection of DNA and thrombin, Nanotechnology 25 (2014) 415501.

[41] C. Pezard, P. Berche, M, Mock, Contribution of individual toxin components to virulence of bacillus anthracis, Infect. Immun. 59 (1991) 3472-3477.

[42] T. A. Taton, C. A. Mirkin, R. L. Letsinger, Scanometric DNA array detection with nanoparticle probes, Science 289 (2000) 1757-1760.

[43] J.-M. Nam, S. I. Stoeva, and C. A. Mirkin, Bio-bar-code-based DNA detection with PCR-like sensitivity, J. Am. Chem. Soc. 126 (2004) 5932-5933.

[44] E. K. Kurbanov, T.-L. Chiu, J. Solberg, S. Francis, K. M. Maize, J. Fernandez, R. L. Johnson, J. E. Hawkinson, M. A. Walters, B. C. Finzel, and E. A. Amin, Probing the S2′ Subsite of the Anthrax Toxin Lethal Factor Using Novel N-Alkylated Hydroxamates, J. Med. Chem. 58 (2015) 8723-8733.

[45] Famous Cases and Criminals (accessed July 23, 2015) (https://www.fbi.gov/about-us/history/famous-cases/anthrax-amerithrax).

[46] P. A. Chopra, S. A. Boone, X. D. Liang, N. S. Duesbery, Anthrax lethal factor proteolysis and inactivation of MAPK kinase, J. Biol. Chem. 278 (2003) 9402-9406.

[47] S. Y. Liu, H. Zhang, Y. Qiao, X. G. Su, One-pot synthesis of ternary $CuInS_2$ quantum dots with near-infrared fluorescence in aqueous solution, RSC Advances 2 (2012) 819-825.

[48] M. Grabolle, M. Spieles, V. Lesnyak, N. Gaponik, A. Eychmüller, U. Resch-Genger,

Determination of the fluorescence quantum yield of quantum dots: suitable procedures and achievable uncertainties, Anal. Chem. 81 (2009) 6285-6294.

[49] Y. Gao, Y. Li, L. Zhang, H. Huang, J. J. Hu, S. M. Shah, X. G. Su, Adsorption and removal of tetracycline antibiotics from aqueous solution by graphene oxide, J. Colloid Interface Sci. 368 (2012) 540-546.

[50] V. L. Pecoraro, J. D. Hermes, W. W. Cleland, Stability constants of magnesium and cadmium complexes of adenine nucleotides and thionucleotides and rate constants for formation and dissociation of magnesium-ATP and magnesium-ADP, Biochemistry 23 (1984) 5262-5271.

[51] N. Ma, G. Tikhomirov, S. O. Kelley, Nucleic acid-passivated semiconductor nanocrystals: biomolecular templating of form and function, Acc. Chem. Res. 43 (2010) 173-180.

[52] T. G. Cha, B. A. Baker, J. Salgado, C. J. Bates, K. H. Chen, A. C. Chang, M. C. Akatay, J. H. Han, M. S. Strano, J. H. Choi, Understanding oligonucleotide-templated nanocrystals: growth mechanisms and surface properties, ACS Nano 6 (2012) 8136-8143.

[53] H. Chang, L. Tang, Y. Wang, J. Jiang, J. Li, Graphene fluorescence resonance energy transfer aptasensor for the thrombin detection, Anal. Chem. 82 (2010) 2341-2346.

[54] N. Varghese, U. Mogera, A. Govindaraj, A. Das, P. K. Maiti, A. K. Sood, C. N. R. Rao, Binding of DNA nucleobases and nucleosides with graphene, ChemPhysChem 10 (2009) 206-210.

[55] Y. Guo, L. Deng, J. Li, S. Guo, E. Wang, S. Dong, Hemin-graphene hybrid nanosheets with intrinsic peroxidase-like activity for label-free colorimetric detection of single-nucleotide polymorphism, ACS Nano 5 (2011) 1282-1290.

[56] C. P. Huang, Y. K. Li and T. M. Chen, A highly sensitive system for urea detection by using CdSe/ZnS core-shell quantum dots, Biosens. Bioelectron. 22 (2007) 1835-1838.

[57] F. Ortmann, W.G. Schmidt, F. Bechstedt, Attracted by long-range electron correlation: adenine on graphite, Phys. Rev. Lett. 95 (2005) 186101.

[58] S. Gowtham, R.H. Scheicher, R. Ahuja, R. Pandey, S.P. Karna, Physisorption of nucleobases on graphene: density-functional calculations, Phys. Rev. B: Condens. Matter Mater. Phys. 76 **(**2007) 033401.

[59] J. Antony, S. Grimme, Structures and interaction energies of stacked graphenenucleobase complexes, Phys. Chem. Chem. Phys. 10 (2008) 2722-2729.

[60] P. J. J. Huang, R. Kempaiah, J. Liu, Synergistic pH effect for reversible shuttling aptamer-based biosensors between graphene oxide and target molecules, J. Mater. Chem. 2011, 21, 8991-8993.

[61] Y. Gao, Y. Li, X. Zou, H. Huang, X. G. Su, Highly sensitive and selective detection of biothiols using graphene oxide-based“molecular beacon”-like fluorescent probe, Analytica Chimica Acta 2012, 73, 68-74.

[62] L. H. Wang, K. Y. Pu, J. Li, X. Y. Qi, H. Li, H. Zhang, C. H. Fan, B. Liu, A graphene-conjugated oligomer hybrid probe for light-up sensing of lectin and *Escherichia Coli*, Adv Mater 2011, 23, 4386-4391.

[63] Z. P. Liu, C. S. Tian, L. H. Lu and X. G. Su, A novel aptamer-mediated $CuInS_2$ quantum dots@graphene oxide nanocomposites-based fluorescence “turn off–on” nanosensor for highly sensitive and selective detection of kanamycin, RSC Adv. 2016, 6, 10205-10214.

Captions:

Scheme 1 (A) The schematic illustration of the preparation of DNA-$CuInS_2$ QDs by a one-step synthesis method, and its use for *anthrax lethal factor* DNA detection, (B) chemical structure of the phosphorothioates and functional domain.

Fig. 1 (A) The TEM images of the $CuInS_2$ QDs (inset: the amplification of a single particle); (B) The TEM images of the DNA-$CuInS_2$ QDs (inset: the amplification of a single particle); (C) The granulometric distribution of $CuInS_2$ QDs; (D) The granulometric distribution of DNA-$CuInS_2$ QDs, respectively; (E) The UV-Vis absorption spectra and normlized fluorescence emission spectra of DNA-$CuInS_2$ QDs (solid line) and $CuInS_2$ QDs (dash line); (F) The photographs of

$CuInS_2$ QDs (left) and DNA-$CuInS_2$ QDs (right) under UV light under the same condition.

Fig. 2 The FT-IR spectra of the L-Cys-capped $CuInS_2$ QDs (green curve) and DNA-$CuInS_2$ QDs (red curve).

Fig. 3 (A) The photostability experiment of the DNA-$CuInS_2$ QDs in aqueous solution with a 590 nm excitation source; (B) The effect of pH on the fluorescence intensity of DNA-$CuInS_2$ QDs after incubation of 60 min.; (C) The effect of salt concentration on the fluorescence intensity of DNA-$CuInS_2$ QDs after incubation of 60 min.

Fig. 4 Fluorescence spectra of DNA-$CuInS_2$ QDs (curve a), the ssDNA-$CuInS_2$ QDs/GO mixture (curve b) and the dsDNA-QDs/GO mixture (curve c). Conditions: 200 μL DNA-$CuInS_2$ QDs, 10 $mmol \cdot L^{-1}$ NaH_2PO_4-Na_2HPO_4 buffer solution containing 100 $\mu mol \cdot L^{-1}$ NaCl, pH 7.4, 0.733 $nmol \cdot L^{-1}$ DNA T1, 1 h for hybridization, 18.0 $\mu g \cdot mL^{-1}$ GO, 30 min for fluorescence quenching.

Fig. 5 (A) Effect of incubation time on the fluorescence intensity of ssDNA-$CuInS_2$ QDs with the addition of GO. I_0 and I were the fluorescence intensity of ssDNA-QDs in the absence and presence of GO, respectively. (B) Effect of incubation time on the fluorescence intensity of dsDNA-QDs with the addition of GO. (C) The relationship between the relative fluorescence intensity I/I_0 and pH. (D) The relationship between the relative fluorescence intensity I/I_0 and salt concentration. I_0 and I were the fluorescence intensity of ssDNA-$CuInS_2$ QDs/GO in the absence and presence of *anthrax lethal factor* DNA, respectively. Conditions: 200 μL DNA-$CuInS_2$ QDs, 10 $mmol \cdot L^{-1}$ NaH_2PO_4-Na_2HPO_4 buffer solution, 0.733 $nmol \cdot L^{-1}$ DNA T1, 1 h for hybridization, 18.0 $\mu g \cdot mL^{-1}$ GO, 30 min for fluorescence quenching. All the RSD values were less than 5.0% (Mean of three replicates).

Fig. 6 The effects of GO concentration on the fluorescence spectra of DNA-$CuInS_2$ QDs system.

Inset: The relationship between I/I_0 and the concentration of GO (from 0 to 18.0 μg·mL^{-1}). I_0 and I were the fluorescence intensity of DNA-$CuInS_2$ QDs in the absence and presence of GO, respectively. (Top to bottom) The concentrations of GO is 0, 0.63, 1.25, 2.51, 3.76, 5.01, 6.27, 7.52, 8.77, 10.00, 11.28, 12.53, 13.78, 15.03, 16.28 and 18.0 μg·mL^{-1}, respectively. Conditions: 10 mmol·L^{-1} NaH_2PO_4-Na_2HPO_4 buffer solution containing 100 μmol·L^{-1} NaCl, pH 7.4, 200 μL DNA-$CuInS_2$ QDs, 30 min for fluorescence quenching. All the RSD values were less than 5.0% (Mean of three replicates).

Fig. 7 Fluorescence spectra of DNA-$CuInS_2$ QDs with different concentrations of DNA T1 in the presence of GO: (a) 0 nmol·L^{-1}, (b) 0.029 nmol·L^{-1}, (c) 0.073 nmol·L^{-1}, (d) 0.117 nmol·L^{-1}, (e) 0.147 nmol·L^{-1}, (f) 0.220 nmol·L^{-1}, (g) 0. 293 nmol·L^{-1}, (h) 0.367 nmol·L^{-1}, (i) 0.440 nmol·L^{-1}, (j) 0.513 nmol·L^{-1}, (k) 0.587 nmol·L^{-1}, (l) 0.660 nmol·L^{-1}, (m) 0.733 nmol·L^{-1}, (n) 0.806 nmol·L^{-1} (o) 0.879 nmol·L^{-1} and (p) 0.952 nmol·L^{-1}, respectively. **Inset**: The relationship between fluorescence intensity ratio I/I_0 and the concentration of DNA T1 in the range of 0.029-0.733 nmol·L^{-1}. I_0 is the original fluorescence intensity of DNA-$CuInS_2$ QDs, and I is the fluorescence intensity of DNA-$CuInS_2$ QDs/GO with the addition of various concentrations of DNA T1. Conditions: 200 μL DNA-$CuInS_2$ QDs, 10 mmol·L^{-1} NaH_2PO_4-Na_2HPO_4 buffer solution containing 100 μmol·L^{-1} NaCl, pH 7.4, 0.733 nmol·L^{-1} DNA T1, 1 h for hybridization, 18.0 μg·mL^{-1} GO, 30 min for fluorescence quenching. All the RSD values were less than 5.0% (Mean of three replicates).

Fig. 8 (A) The corresponding fluorescence intensity ratio (I/I_0) histograms in the presence of DNA target T1 (red bar), single-base-mismatched target DNA T2 (green bar) and two-base-mismatched target DNA T3 (blue bar). I and I_0 were the fluorescence intensity of DNA-$CuInS_2$ QDs with and without T1, T2 or T3 in the presence of GO, respectively; (B) The fluorescence intensity of

dsDNA-$CuInS_2$ QDs/GO solution and dsDNA-$CuInS_2$ QDs/GO solution with coexisting ions and molecules (K^+, Na^+, Ca^{2+}, Mg^{2+}, Zn^{2+}, acetate, Cl^-, SO_4^{2-}, CO_3^{2-}, citrate, glucose, BSA and HSA). Conditions: 200 μL DNA-$CuInS_2$ QDs, 10 mmol·L^{-1} NaH_2PO_4-Na_2HPO_4 buffer solution containing 100 μmol·L^{-1} NaCl, pH 7.4, 0.733 nmol·L^{-1} DNA T1, T2, T3; 1 h for hybridization, 18.0 μg·mL^{-1} GO, 30 min for fluorescence quenching. All the RSD values were less than 5.0% (Mean of three replicates).

Table 1 Determination of *anthrax lethal factor* DNA in human serum samples according to equation (1)

Figures:

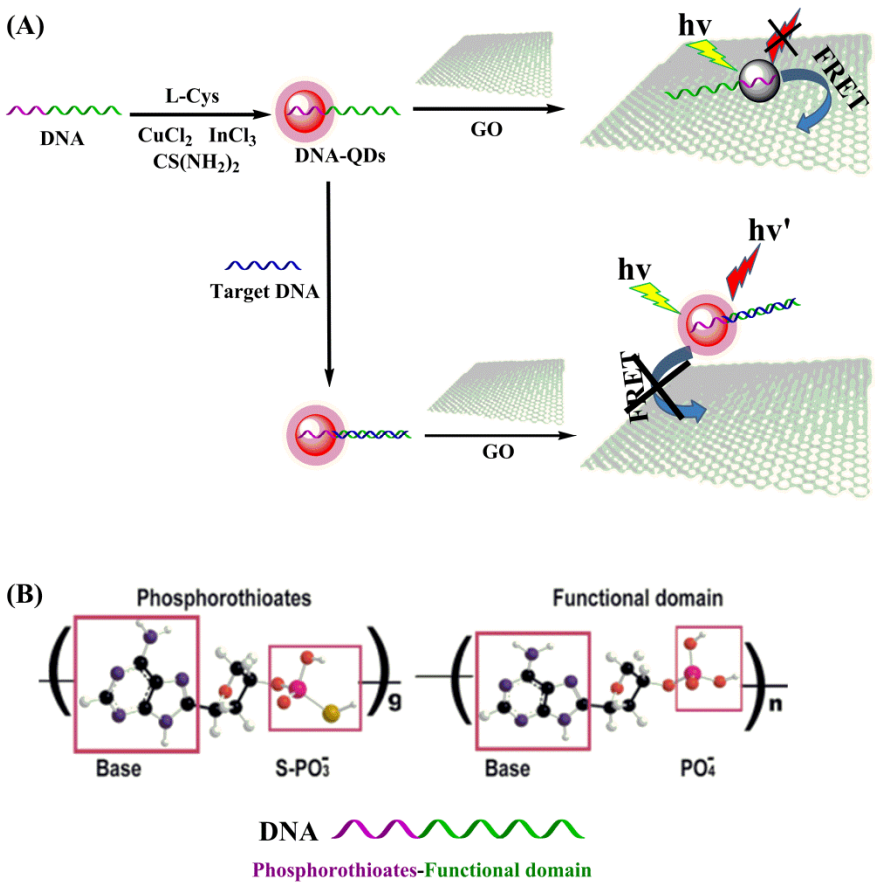

Scheme 1

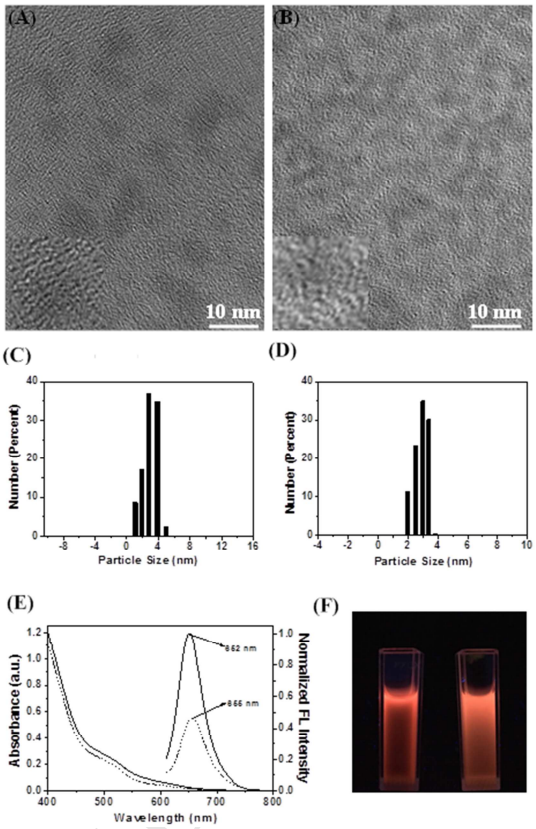

Fig. 1

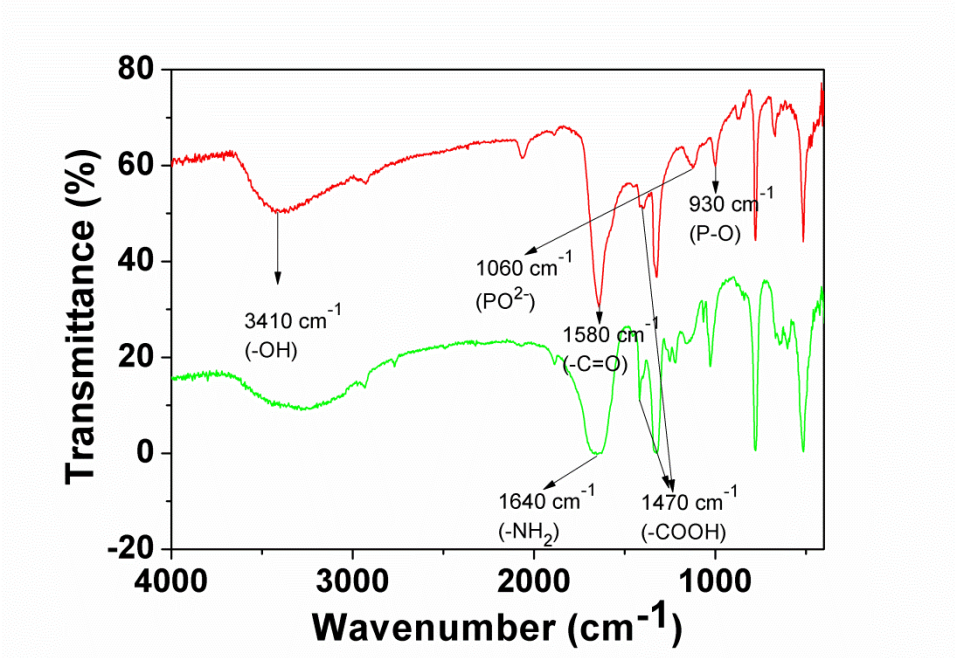

Fig. 2

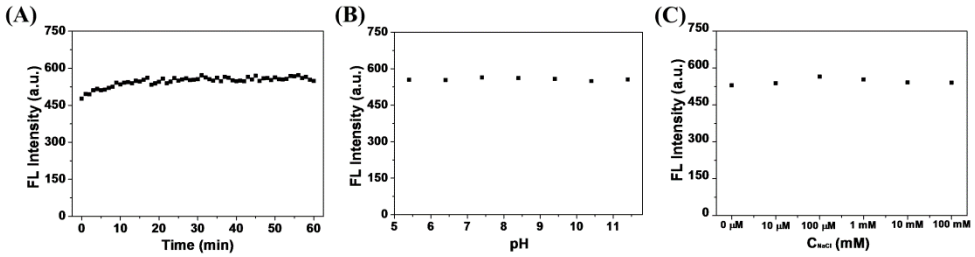

Fig. 3

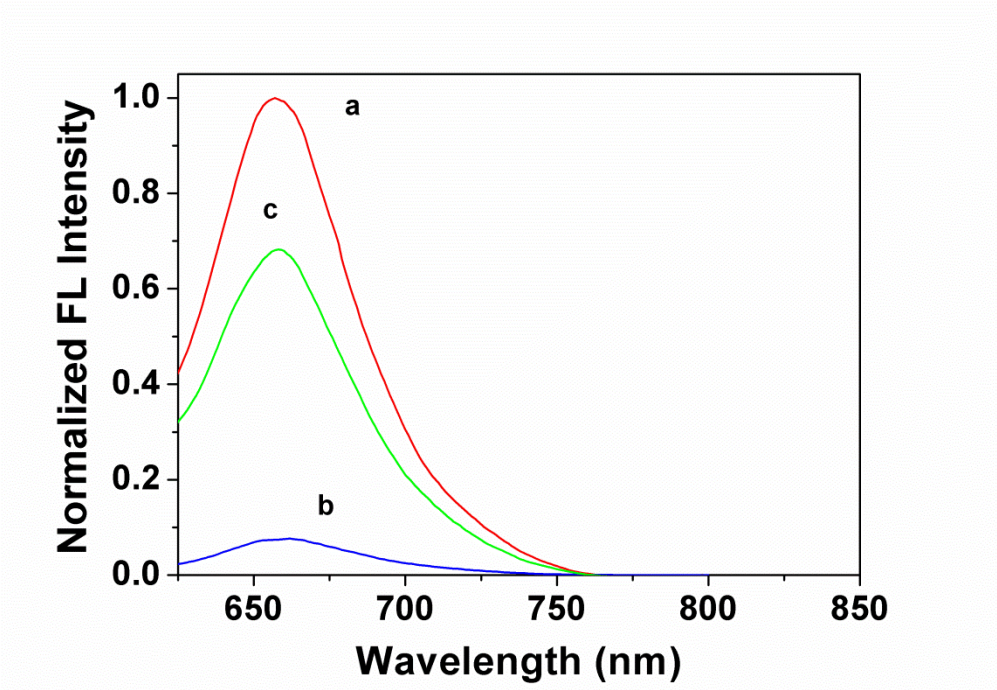

Fig. 4

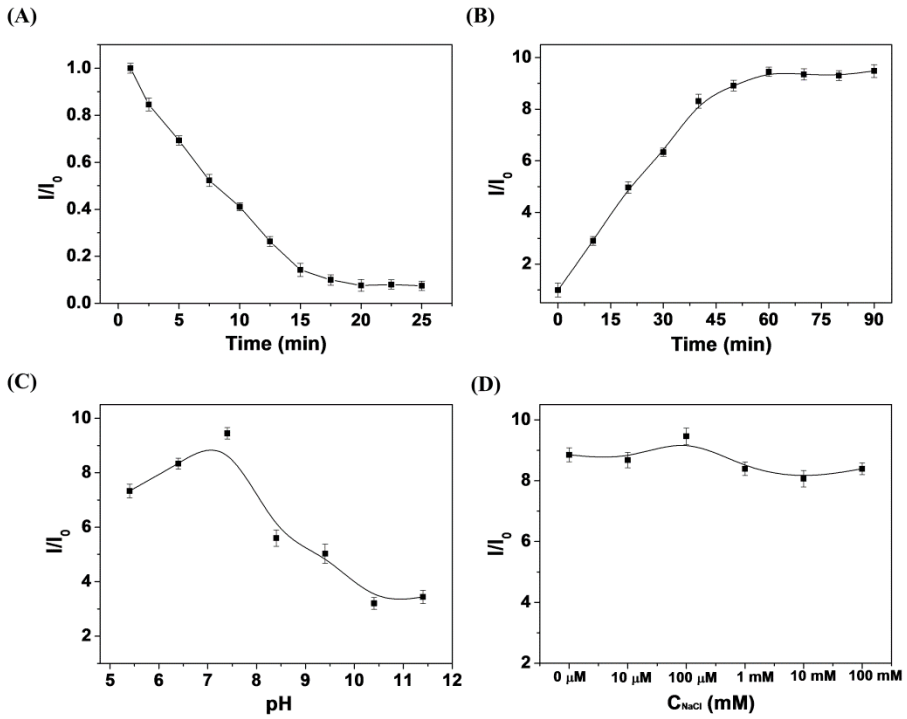

Fig. 5

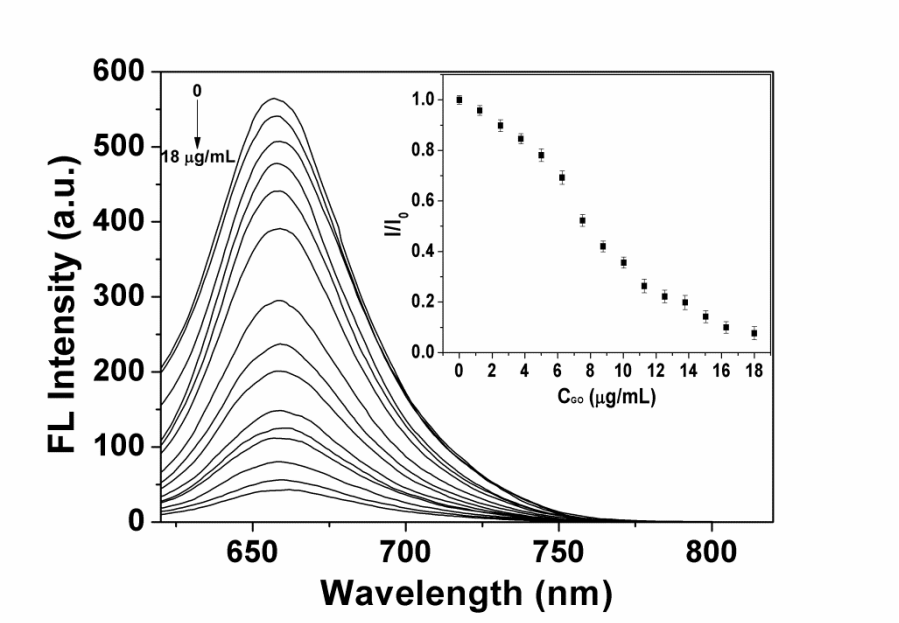

Fig. 6

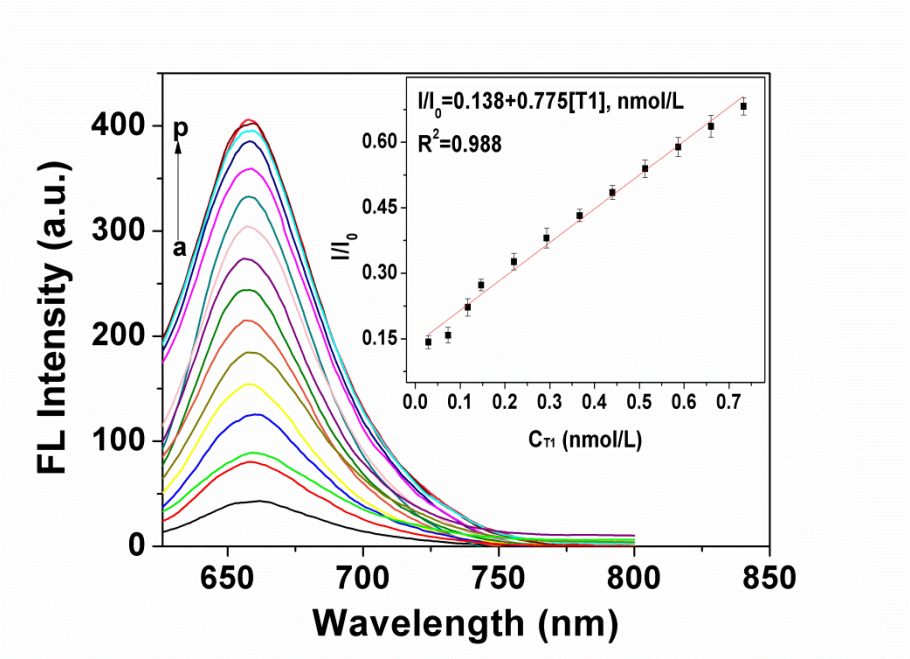

Fig. 7

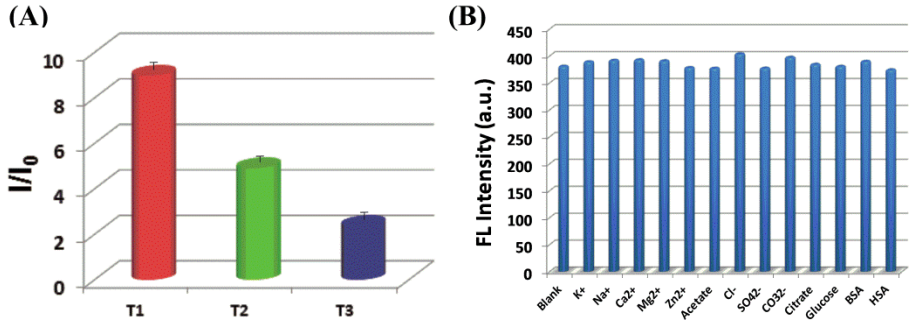

Fig. 8

Table 1 Determination of *anthrax lethal factor* DNA in human serum samples according to equation (1)

Sample	Added (nM)	Found (nM)	Recovery (%)	RSD (n=3, %)
1	0.05	0.048	96.0	2.00
2	0.10	0.099	99.0	1.33
3	0.20	0.210	105.0	3.25

Highlights:

► Strongly fluorescent DNA-$CuInS_2$ QDs were successfully prepared by a one-pot hydrothermal method with fluorescence quantum yield as high as 23.4%.

► A novel fluorescent biosensor for label-free detection of *anthrax lethal factor* DNA was established based on the as-prepared DNA-$CuInS_2$ QDs.

► The DNA sensor took advantage of the feature that single-stranded DNA binds to GO with significantly higher affinity than double-stranded DNA.

► Good sensitivity and selectivity were obtained.

► This method was utilized to detect *anthrax lethal factor* DNA in real sample with satisfactory results.